

SCIENTIFIC REPORTS



OPEN

Synthesis of the extended phenacene molecules, [10]phenacene and [11]phenacene, and their performance in a field-effect transistor

Hideki Okamoto¹, Shino Hamao², Ritsuko Eguchi², Hidenori Goto², Yasuhiro Takabayashi¹, Paul Yu-Hsiang Yen³, Luo Uei Liang³, Chia-Wei Chou³, Germar Hoffmann³, Shin Gohda⁴, Hisako Sugino⁴, Yen-Fa Liao⁵, Hirofumi Ishii⁵ & Yoshihiro Kubozono²

The [10]phenacene and [11]phenacene molecules have been synthesized using a simple repetition of Wittig reactions followed by photocyclization. Sufficient amounts of [10]phenacene and [11]phenacene were obtained, and thin-film FETs using these molecules have been fabricated with SiO₂ and ionic liquid gate dielectrics. These FETs operated in p-channel. The averaged measurements of field-effect mobility, $\langle\mu\rangle$, were $3.1(7) \times 10^{-2}$ and $1.11(4) \times 10^{-1} \text{ cm}^2 \text{ V}^{-1} \text{ s}^{-1}$, respectively, for [10]phenacene and [11]phenacene thin-film FETs with SiO₂ gate dielectrics. Furthermore, [10]phenacene and [11]phenacene thin-film electric-double-layer (EDL) FETs with ionic liquid showed low-voltage p-channel FET properties, with $\langle\mu\rangle$ values of 3(1) and 1(1) $\text{cm}^2 \text{ V}^{-1} \text{ s}^{-1}$, respectively. This study also discusses the future utility of the extremely extended π -network molecules [10]phenacene and [11]phenacene as the active layer of FET devices, based on the experimental results obtained.

The chemistry and physics of extended π -network molecules such as fullerene, graphite/graphene, and conjugated organic polymers/hydrocarbons are currently one of the most interesting and challenging frontiers of fundamental science, because these molecules have displayed excellent performance in electronics applications, as well as novel physical properties such as superconductivity^{1–28}. The study of electronics using conjugated organic molecules has made rapid progress, in particular in electronics such as field-effect transistors (FETs) and solar cells^{9–11,13–16,18–23,26–28}.

Our study of the fabrication and characterization of FETs using phenacene molecules, which consist of coplanar fused benzene rings in a repeating W-shaped pattern, has demonstrated excellent FET properties^{19,23,26–28}. This high performance is due to the strong π - π interaction between phenacene molecules enabled by the extension of the benzene network. Showing a clear pattern, the field-effect mobility, μ , which is an indication of FET performance, has increased with the number of benzene rings, n ; we have already synthesized phenacene molecules with 5–9 benzene rings, *i.e.*, picene to [9]phenacene^{19,26–28}. Thus the next step was to synthesize phenacene molecules with more than 9 benzene rings, and to fabricate FETs with the molecules. This was challenging because of the difficulty in synthesis caused by their quite low solubility in organic solvents; a low solubility often fatal in organic synthesis. Previously, only alkyl-substituted [11]phenacene^{29,30} and tetracarboxy [n]phenacene ($n = 10, 12$ and 14)³¹ had been synthesized, based for [n]phenacene molecules with $n \geq 10$, but these are phenacene derivatives. No previous synthesis of unsubstituted phenacene molecules with $n \geq 10$ has been reported, although they are quite significant as a matter of basic chemistry, as well as for their potential utility in electronic applications.

¹Department of Chemistry, Okayama University, Okayama, 700-8530, Japan. ²Research Institute for Interdisciplinary Science, Okayama University, Okayama, 700-8530, Japan. ³Department of Physics, National Tsing Hua University, Hsinchu, 30013, Taiwan. ⁴NARD Co Ltd, Amagasaki, 660-0805, Japan. ⁵National Synchrotron Radiation Center, Hsinchu, 30076, Taiwan. Correspondence and requests for materials should be addressed to Y.K. (email: kubozono@cc.okayama-u.ac.jp)

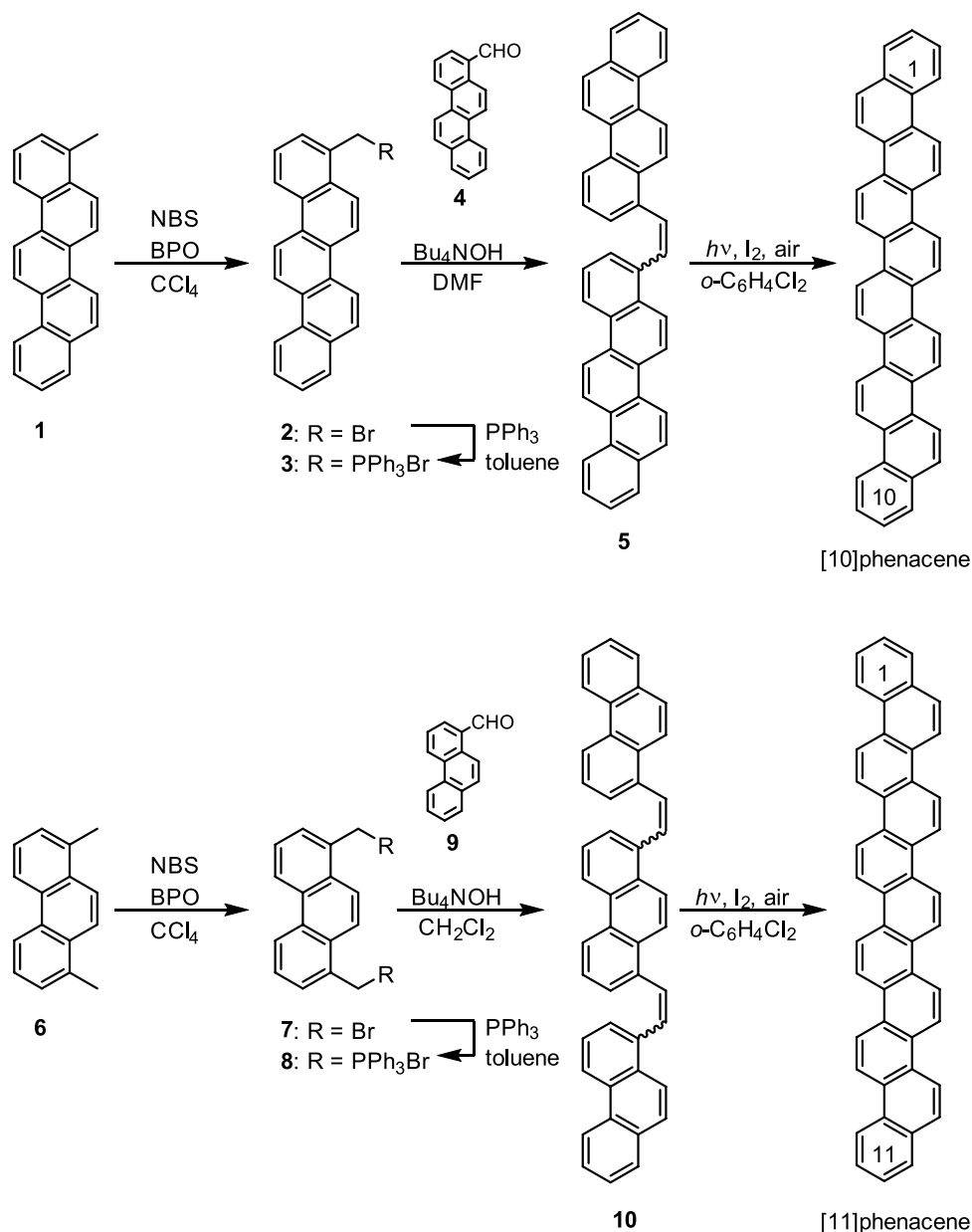


Figure 1. Synthetic routes to [10]phenacene and [11]phenacene.

Here, we have synthesized the longest extended π -network molecules to date, [10]phenacene and [11]phenacene, using a simple repetition of Wittig reactions followed by photocyclization^{29–35}. The synthesized samples were fully characterized using MALDI-time-of-flight mass spectrometry (MALDI-TOF MS), X-ray diffraction (XRD), and electronic absorption spectra, which confirmed the identity of these molecules. FET devices were then fabricated using thin films of these molecules, and their FET properties were fully investigated. The structural/electronic parameters of [10]phenacene and [11]phenacene, as well as their FET parameters, have been fully compared with those of other phenacene molecules, and the future prospect for FET application of extremely extended phenacene molecules is discussed.

Results

Preparation and characterization of [10]phenacene and [11]phenacene. The samples of [10]phenacene and [11]phenacene were synthesized as shown in Fig. 1. Experimental details are described in the Method section. The key step for synthesizing large phenacene molecules is based on the photocyclization of diarylethene^{29–35}, known as the Mallory photocyclization, followed by oxidative aromatization to form a phenanthrene-like zigzag benzene array. Diarylethene 5, which is the precursor to [10]phenacene, was prepared by a Wittig reaction between phosphonium salt 3 and chrysenecarbaldehyde 4 using tetrabutylammonium hydroxide (Bu₄NOH) as base. The diarylethene 5 was used in the Mallory photocyclization without separation of *E*- and *Z*-isomers; the crude diarylethene 5 was photolyzed at 365 nm in *o*-dichlorobenzene at ca. 150 °C in the presence

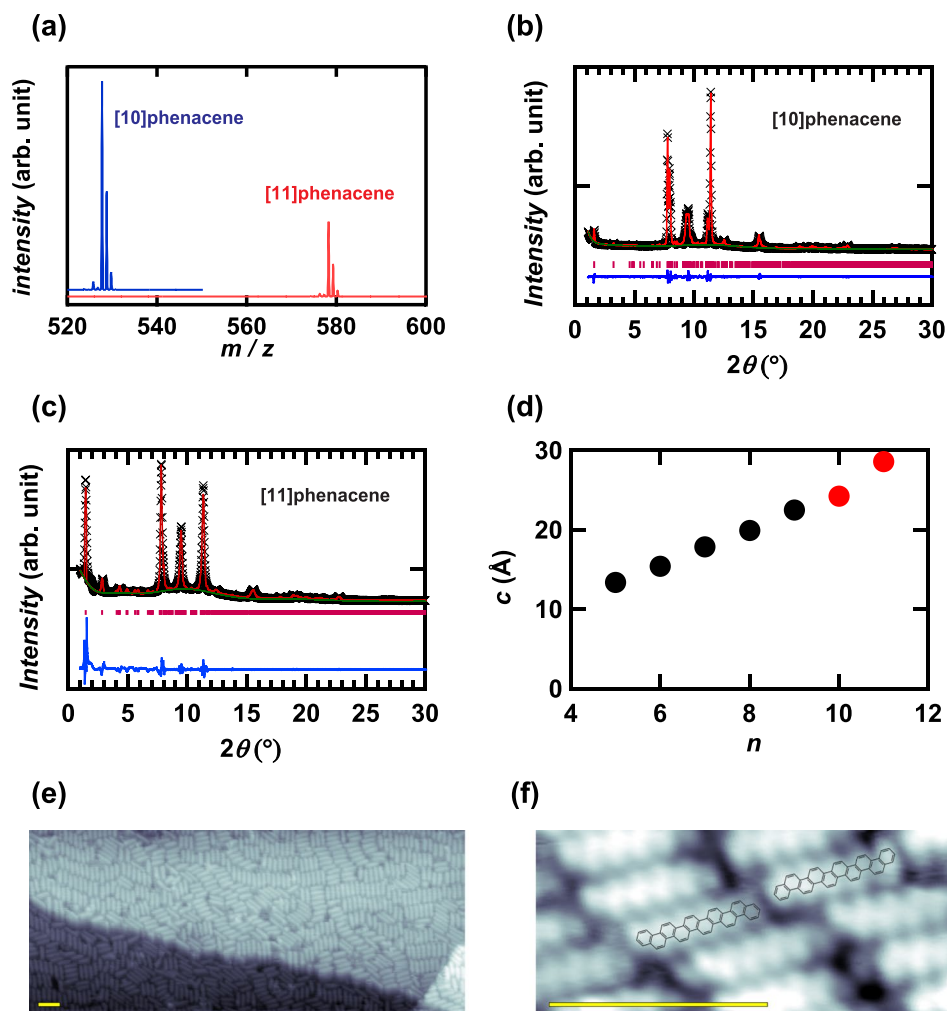


Figure 2. (a) MALDI-TOF MS spectra of [10]phenacene and [11]phenacene samples. XRD patterns of powder samples of (b) [10]phenacene and (c) [11]phenacene. (d) $c-n$ plots of [n]phenacenes with $n = 5-11$. The 'x' plot and red line refer to the experimental and the calculated patterns, respectively, in (b) and (c). The red bar and blue line correspond to the position of Bragg reflection and the difference between the experimental and the calculated patterns. (e) STM image of 0.9 ML of [10]phenacene molecules deposited on Au substrate, and (f) the expanded STM image. The scale indicated by yellow bars ((e) and (f)) corresponds to 5 nm. The 10-lobes are shown in the STM image.

of a catalytic amount of I_2 to produce [10]phenacene as an off-white precipitate, which was simply collected by filtration. [11]Phenacene was prepared by a Wittig reaction between bis-phosphonium salt **8** and phenanthrenecarbaldehyde **9**, followed by a two-fold Mallory photocyclization of the resulting diene **10** in boiling *o*-dichlorobenzene. Because precursors **5** and **10** were hardly soluble in common organic solvents, their Mallory photocyclization was carried out at elevated temperatures.

The [10]phenacene and [11] phenacene molecules were characterized by elemental analyses, their MALDI-TOF MS spectra (Fig. 2a) and powder XRD patterns (Fig. 2b,c). The elemental analyses showed the values of 95.26% for C and 4.36% for H for [10]phenacene where the calculated values are 95.42% for C and 4.58% for H, while the values of 95.07% for C and 4.48% for H for [11]phenacene where the calculated values are 95.47% for C and 4.53% for H. The MS spectra showed peaks at $m/z = 527.73$, 528.78 and 529.76 for [10]phenacene, and $m/z = 578.26$, 579.29 and 580.29 for [11]phenacene, respectively, indicating the successful synthesis of these molecules. The splitting of peaks reflects the natural abundance of isotopes of C and H in [10]phenacene ($C_{42}H_{24}$) and [11]phenacene ($C_{46}H_{26}$). The powder XRD patterns of [10]phenacene and [11]phenacene were analyzed by Le Bail fitting under the space group $P2_1$ (monoclinic, No. 4). The lattice constants of [10]phenacene, a , b , c , and β , were determined to be 8.5416(7), 6.2281(5), 24.2227(6) Å, and 93.031(4)°, respectively, while those of [11]phenacene were determined to be 9.893(6), 6.097(2), 28.587(5) Å, and 90.83(2)°, respectively.

Here, it is noticed that single crystal XRD measurement could not be achieved because of no success in preparation of single crystals of [10]phenacene and [11]phenacene in this study. In addition, it has been difficult to achieve the single crystal XRD measurement because of the formation of very thin single crystals (plate-shape) for phenacene molecules. The single crystal diffraction measurement may be the future work. Nevertheless,

successful synthesis of [10]phenacene and [11]phenacene was evidenced employing the methods described above, as well as those shown below.

The $c - n$ plot is shown in Fig. 2d, in which n refers to the number of benzene rings. The c value straightforwardly increases with the increase in n , suggesting the elongation of the phenacene framework, additional evidence that molecules of [10]phenacene and [11]phenacene were in fact synthesized. We have obtained more than 30 mg of samples of [10]phenacene and [11]phenacene. This is the first success in obtaining macroscopic amounts of solid samples of the above molecules.

Direct evidence of the molecular structure is given by scanning tunnelling microscope (STM) experiments. [10]phenacene molecules were thermally deposited on an Au(111) surface with ~90% coverage; with less coverage, molecules remain mobile, and the instability renders imaging infeasible. Figure 2e presents a representative large-scale image of [10]phenacene molecules on Au terraces separated by monoatomic Au steps, one running from the left to the right and one located in the bottom right corner. The molecules are closely aggregated in small grains with different orientations, their molecular planes parallel to the Au surface.

As depicted in Fig. 2f, a closer inspection of the single molecule structure reveals a pronounced internal 10-lobe structure, with each lobe corresponding to one of ten benzene rings. This STM image clearly corresponds to a [10]phenacene molecule. Two mirror-symmetric pairs are observed, as shown in Fig. 2f, which is consistent with the result for other $[n]$ phenacene molecules³⁶. The growth of the [10]phenacene layer starts with the physisorption of a [10]phenacene molecule on the Au surface, which is characteristic of non-polar molecules deposited on an Au(111) surface. The STM image makes it clear that [10]phenacene molecules are deposited without any thermal damage. This fact is significant because thermal deposition of [10]phenacene and [11]phenacene molecules was used to form thin films as active layers of FET devices. The study on STM of [11]phenacene molecule would be the future work because obtaining the clear STM image requires much time and effort, although it is not shown in this study.

Figure 3a,b show out-of-plane XRD patterns for thin films of [10]phenacene and [11]phenacene, respectively, which were prepared on a SiO₂/Si substrate by thermal deposition, as described in the Method section. The peaks due to $00l$ were observed for these thin films, as seen from Fig. 3a,b. This means that the ab planes in both thin films are parallel to the substrate. The value of the inverse absolute reciprocal of c , $1/|c^*|$, which corresponds to the distance between ab -layer planes, d_{001} , was determined from each thin film. The average values, $\langle 1/|c^*| \rangle = \langle d_{001} \rangle$, were evaluated to be 25(1) and 19.5(2) Å for [10]phenacene and [11]phenacene, respectively. The $\langle d_{001} \rangle - n$ plot is shown in Fig. 3c. The $\langle d_{001} \rangle$ increases straightforwardly with increasing n , up to $n = 10$, indicating that the angle between the long axis of the molecule and c^* , ϕ , is almost the same among phenacene molecules with $n \leq 10$; the ϕ is schematically depicted in Fig. 3d. Actually, as seen from Fig. 3e, the ϕ value slowly decreases with n . Then the $\langle d_{001} \rangle$ value (=19.5(2) Å) for [11]phenacene is much smaller than that (=25(1) Å) of [10]phenacene despite the larger long axis in [11]phenacene. This suggests two possibilities: (1) [11]phenacene was broken by thermal deposition, (2) The ϕ value for [11]phenacene deviates significantly from the trend of ϕ -versus- n , in which ϕ slowly decreases against n over the range $n \leq 10$ ($\phi = 10\text{--}30^\circ$)²⁸. The ϕ for [10]phenacene was 10° , which is consistent with the above tendency. If the second scenario is the complete explanation, the ϕ value of [11]phenacene is estimated to be 45° . This value is inconsistent with the scenario that the strengthening of π - π interaction accompanied by an increase in π -framework must provide progressively smaller ϕ ²⁸. Thus, the reason why the ϕ changes drastically at $n = 11$ remains to be clarified, but the decomposition of [11]phenacene during thermal deposition would be neglected, because of significant experimental evidence as described below.

Figure 4a shows the UV-VIS absorption spectra for thin films of phenacene molecules with $n = 5\text{--}11$. All spectra show a similar pattern, and the first peak at 3.0–3.5 eV shifts systematically to lower energy, which indicates that the first electron excitation energy decreases with n , *i.e.*, the band gap becomes narrower against n as n increases from 5 to 11, in the same manner as the band gap versus n at $n = 5\text{--}9$ reported previously²⁸. The similarity in UV-VIS absorption spectra for thin films of each phenacene molecule suggests that the [11]phenacene molecule is not broken even in a thin film, *i.e.*, by thermal deposition. The onset energy, $E(\text{onset})$, of the absorption spectrum, which corresponds to the band gap, is plotted as a function of n (Fig. 4b). The energy for highest occupied molecular orbital (HOMO) was determined for [10]phenacene and [11]phenacene thin films using photoelectron yield spectrum (PYS), and the energy of lowest unoccupied molecular orbital (LUMO) was determined from the energy of HOMO level and band gap (HOMO-LUMO gap). The HOMO and LUMO levels are shown in Fig. 4c, indicating that the HOMO level lowers gradually up to $n = 11$. This would be also the evidence for no decomposition (or destruction) of sample. Thus, the successful synthesis of [10]phenacene and [11]phenacene led to the systematic elucidation of structural and electronic features of extended phenacene molecules.

Fabrication and transport characteristics of FET devices using thin films of [10]phenacene and [11]phenacene.

No studies on the FET characteristics of [10]phenacene and [11]phenacene FET devices have been reported to date. At the present stage, an FET device using a thin film of the most extended π -network molecule was fabricated using [9]phenacene²⁸. Because of difficulty in synthesis, macroscopic amounts of [10]phenacene and [11]phenacene had not yet been obtained, and the FET application of such π -extended molecules was not possible. In this study, FET devices with thin films of [10]phenacene and [11]phenacene were fabricated, in which 400 nm thick SiO₂ was employed as the gate dielectric. Figure S1a of Supplementary Information shows the FET device structure, and atomic force microscope (AFM) images of thin films of [10]phenacene and [11]phenacene are shown in Fig. S1b and c, respectively, images of the samples that were used for the active layers of FET devices. The rough surface on the thin films of [10]phenacene and [11]phenacene, and the root mean square (RMS) roughness are 6.2 and 9.7 nm, respectively; probably because of the length of the molecule (or large $\langle d_{001} \rangle$).

The transfer and output characteristics of a [10]phenacene thin-film FET are shown in Fig. 5a,b, respectively, displaying its p-channel normally-off FET properties. The field-effect mobility, μ , absolute threshold

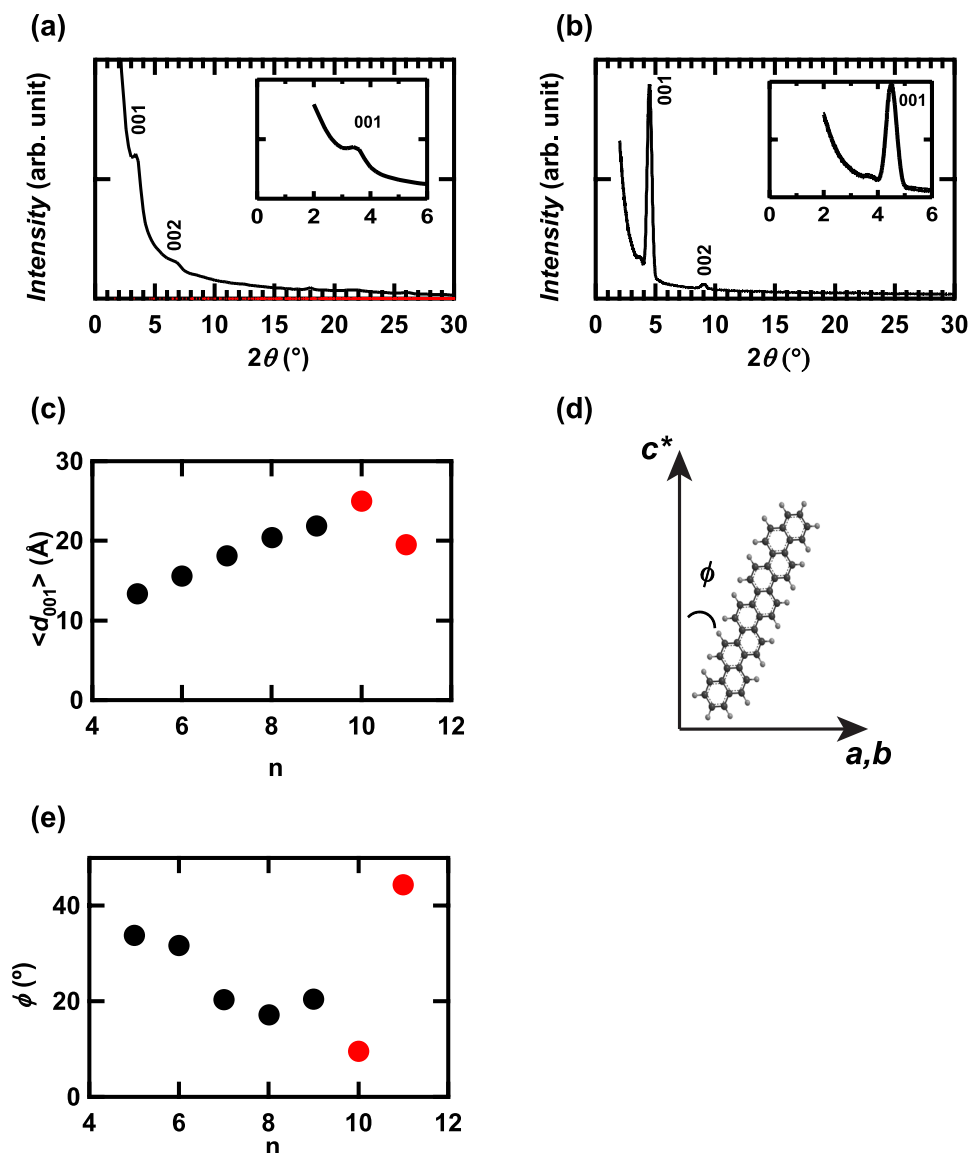


Figure 3. Out-of-plane XRD patterns of thin films of (a) [10]phenacene and (b) [11]phenacene. (c) $\langle d_{001} \rangle$ - n plot of [n]phenacene at n = 5–11. The inclined angle, ϕ , of an [n]phenacene molecule with respect to c^* is schematically shown in (d). (e) ϕ - n plot of [n]phenacene at n = 5–11.

voltage, $|V_{th}|$, on-off ratio and subthreshold swing, S , for the [10]phenacene thin film FET were determined to be $3.70 \times 10^{-2} \text{ cm}^2 \text{ V}^{-1} \text{ s}^{-1}$, 39.0 V, 3.5×10^5 , and $6.5 \text{ V decade}^{-1}$, respectively, from the forward transfer curve (Fig. 5a). The averaged values of these parameters were evaluated from five devices to be $3.1(7) \times 10^{-2}$, 40(1) V, $3(2) \times 10^5$, and $5(1) \text{ V decade}^{-1}$, respectively; the FET parameters of all devices are listed in Table 1. Unfortunately, the averaged μ value ($\langle \mu \rangle$) is smaller than that ($\langle \mu \rangle = 1.2(3) \times 10^{-1} \text{ cm}^2 \text{ V}^{-1} \text{ s}^{-1}$) of a [9]phenacene thin film FET with SiO_2 gate dielectric²⁸.

The transfer and output characteristics of an [11]phenacene thin-film FET are shown in Fig. 5c,d, respectively, showing p-channel normally-off FET properties, as in the [10]phenacene thin-film FET. The values of μ , $|V_{th}|$, on-off ratio and S for an [11]phenacene thin-film FET were determined to be $1.18 \times 10^{-1} \text{ cm}^2 \text{ V}^{-1} \text{ s}^{-1}$, 42.9 V, 3.8×10^5 , and $5.5 \text{ V decade}^{-1}$, respectively, from the forward transfer curve (Fig. 5c). The averaged values of these parameters were evaluated from five devices to be $1.11(4) \times 10^{-1}$, 48(7) V, $4(2) \times 10^5$, and $5(1) \text{ V decade}^{-1}$, respectively; the FET parameters of all devices are listed in Table 2. The $\langle \mu \rangle$ is almost the same as that ($\langle \mu \rangle = 1.2(3) \times 10^{-1} \text{ cm}^2 \text{ V}^{-1} \text{ s}^{-1}$) of a [9]phenacene thin film FET with an SiO_2 gate dielectric²⁸. Finally, we must comment that the FET devices with thin films of [10]phenacene and [11]phenacene operated stably for several months even in air, indicating the stability of these molecules. This is also an advantage of using these molecules as active layers of FET devices.

Here, it should be noted that the high $|V_{th}|$ and large S are observed for the [10]phenacene and [11]phenacene FETs, which are general features of phenacene FETs^{19,21,23,26–28}. The most significant factor for the high $|V_{th}|$ and large S may be the density of trap states contained in thin films, *i.e.*, trap states of hole in p-channel operation such

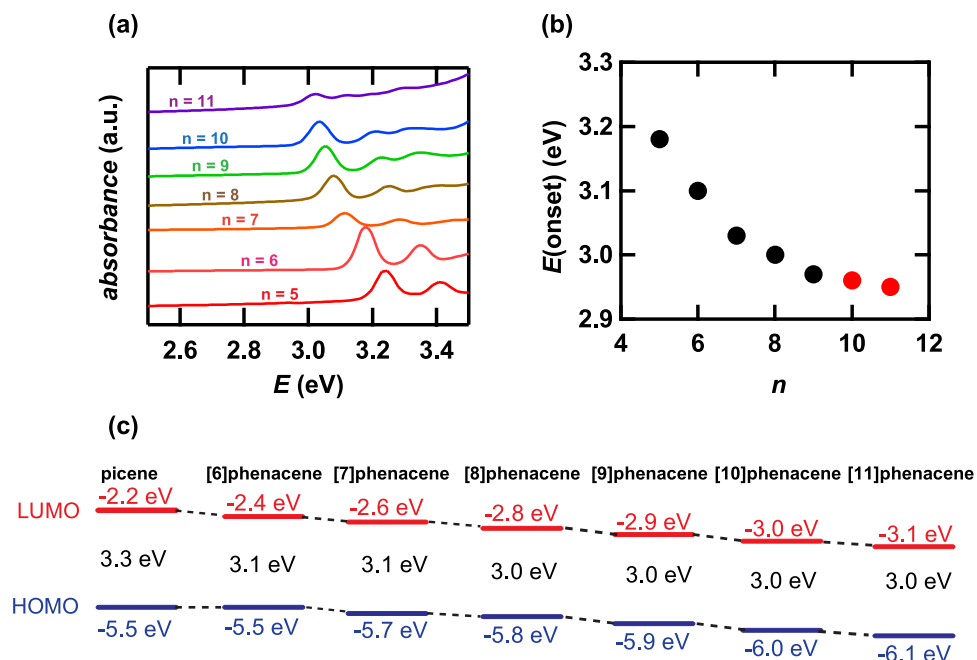


Figure 4. (a) UV-VIS absorption spectra of thin films of [n]phenacene with $n = 5-11$. (b) Onset energy ($E(\text{onset})$) - n plot of [n]phenacene with $n = 5-11$. (c) Energy diagram of [n]phenacene ($n = 5-11$). The numerical value written in black colour refers to the HOMO-LUMO gap.

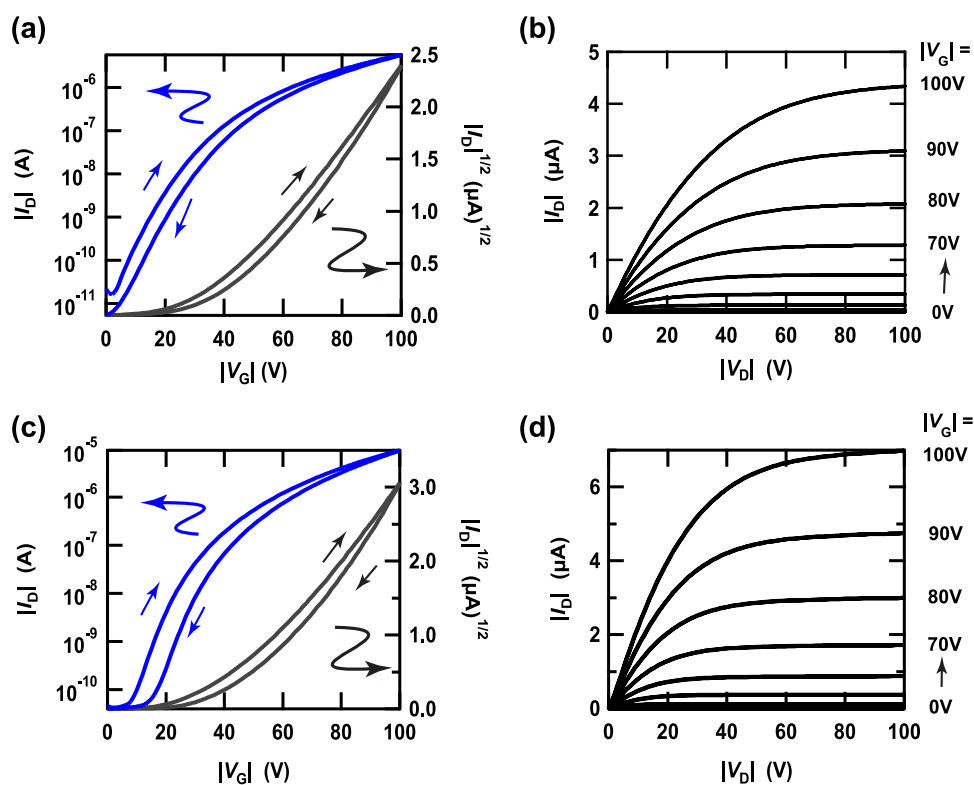


Figure 5. (a) Transfer and (b) output curves of a [10]phenacene thin-film FET with an SiO_2 gate dielectric. (c) Transfer and (d) output curves of an [11]phenacene thin-film FET with an SiO_2 gate dielectric.

as phenacene FET^{37,38}. Therefore, it is important to reduce the trap states or to effectively fill in the trap states by holes for realizing low $|V_{\text{th}}|$ and small S . In the next section, we report low-voltage operation (low $|V_{\text{th}}|$ and small S) in [10]phenacene and [11]phenacene FETs by using EDL capacitor, which means the effective filling of the tarp states by holes.

sample	μ ($\text{cm}^2\text{V}^{-1}\text{s}^{-1}$)	$ V_{\text{th}} $ (V)	ON/OFF	S (V/decade)	L (μm)	W (μm)
#1	3.70×10^{-2}	39.0	3.5×10^5	6.5	50	500
#2	3.54×10^{-2}	41.2	7.3×10^5	4.7	50	500
#3	3.64×10^{-2}	38.6	1.4×10^5	5.9	100	500
#4	2.40×10^{-2}	40.3	2.5×10^5	2.8	450	1000
#5	2.39×10^{-2}	40.9	2.1×10^5	4.8	50	500
average	$3.1(7) \times 10^{-2}$	40(1)	$3(2) \times 10^5$	5(1)	—	—

Table 1. FET parameters of a [10]phenacene thin-film FET with an SiO_2 gate dielectric. The parameters were determined from the forward transfer curves.

sample	μ ($\text{cm}^2\text{V}^{-1}\text{s}^{-1}$)	$ V_{\text{th}} $ (V)	ON/OFF	S (V/decade)	L (μm)	W (μm)
#1	1.182×10^{-1}	42.9	3.8×10^5	5.5	50	500
#2	1.086×10^{-1}	42.7	6.1×10^4	6.1	100	500
#3	1.106×10^{-1}	47.0	3.4×10^5	3.8	150	500
#4	1.072×10^{-1}	49.8	2.8×10^5	5.7	200	500
#5	1.093×10^{-1}	58.8	7.3×10^5	3.5	135	500
average	$1.11(4) \times 10^{-1}$	48(7)	$4(2) \times 10^5$	5(1)	—	—

Table 2. FET parameters of an [11]phenacene thin-film FET with an SiO_2 gate dielectric. The parameters were determined from the forward transfer curves.

Fabrication and transport characteristics of EDL FET devices using [10]phenacene and [11]phenacene. EDL FET devices with thin films of [10]phenacene and [11]phenacene were fabricated with ionic liquid (butyl-3-methylimidazolium hexafluorophosphate: bmim[PF₆]) used for the EDL gate dielectric. The active layer was a thin film of [10]phenacene or [11]phenacene. Figure S1d shows the device structure of the EDL FET device, which employed a top gate dielectric and side gate electrode. The transfer and output characteristics of a [10]phenacene EDL FET are shown in Fig. 6a,b, respectively, showing p-channel normally-off FET properties. The operation voltage was too low in comparison with the device with an SiO_2 gate dielectric (Fig. 5a,b).

The μ , $|V_{\text{th}}|$, on-off ratio and S for the [10]phenacene EDL FET were determined to be $4.2 \text{ cm}^2 \text{ V}^{-1} \text{ s}^{-1}$, 2.18 V, 1.0×10^3 , and $4.0 \times 10^{-1} \text{ V decade}^{-1}$, respectively, from the forward transfer curve (Fig. 6a). Furthermore, the average values of FET parameters were evaluated from five devices to be $3(1) \text{ cm}^2 \text{ V}^{-1} \text{ s}^{-1}$, 2.3(2) V, $2(1) \times 10^3$, and $7(5) \times 10^{-1} \text{ V decade}^{-1}$, respectively; the FET parameters of all devices are listed in Table 3. The FET performance of [10]phenacene EDL FET is quite high.

The transfer and output characteristics of an [11]phenacene EDL FET are shown in Fig. 6c,d, respectively, showing p-channel normally-off FET properties. The operation voltage is also too low in comparison with that using an SiO_2 gate dielectric (Fig. 5c,d). The μ , $|V_{\text{th}}|$, on-off ratio and S for an [11]phenacene EDL FET were determined to be $2.6 \text{ cm}^2 \text{ V}^{-1} \text{ s}^{-1}$, 2.30 V, 1.0×10^7 , and $1.01 \times 10^{-1} \text{ V decade}^{-1}$, respectively, from the forward transfer curve (Fig. 6c). Furthermore, the average values of FET parameters were evaluated from five devices to be $1(1) \text{ cm}^2 \text{ V}^{-1} \text{ s}^{-1}$, 2.3(1) V, $4(4) \times 10^6$, and $1.6(5) \times 10^{-1} \text{ V decade}^{-1}$, respectively; the FET parameters of all devices are listed in Table 4. The FET performance of an [11]phenacene EDL FET is lower than that of a [10]phenacene EDL FET. To sum up, the value of μ is higher in [10]phenacene and [11]phenacene EDL FETs than in the corresponding thin-film FETs with SiO_2 gate dielectric. The $\langle \mu \rangle$ ($=3(1) \text{ cm}^2 \text{ V}^{-1} \text{ s}^{-1}$) in a [10]phenacene EDL FET is larger than that ($=9(2) \times 10^{-1} \text{ cm}^2 \text{ V}^{-1} \text{ s}^{-1}$)²⁸ in a [9]phenacene EDL FET. In addition, these EDL FETs operated stably in Ar-filled glove box for several months, indicating the stability of EDL FET using the thin films of [10]phenacene and [11]phenacene molecules.

Discussion

The extended benzene-network molecules, [10]phenacene and [11]phenacene, were synthesized, and these molecules were employed in a thin-film FET. These molecules consist of 10 and 11 fused benzene rings in a repeating W-shaped structure. No attempts at the synthesis of phenacene molecules with 10 and 11 benzene rings have previously been made because of the difficulties in synthesis. We used the ‘Mallory protocol’^{26–35}, which consists of the simple repetition of a Wittig reaction followed by photocyclization, for the synthesis, which provided sufficient amounts not only to characterize their crystal structure and electronic properties but also to incorporate in FET devices. Thus, the effectiveness of the Mallory homologation protocol for the synthesis of extended π -network molecules was verified in this study.

In particular, the successful synthesis of phenacene molecules without any functional groups is very significant because the molecular framework may not be distorted. While the π -framework of phenacene molecules with functional groups is distorted³³, that of phenacene molecules without functional groups is expected to have a planar structure. This simplifies the study of these extended π -network molecules, *i.e.*, we can truly pursue the electronic nature of the extended π -network molecules and their utility in electronics without the distraction of side issues such as substituent effects and a distorted π -framework. Therefore, this study provides the first step in the study of the chemistry and physics of extremely extended phenacene molecules and their application in electronics.

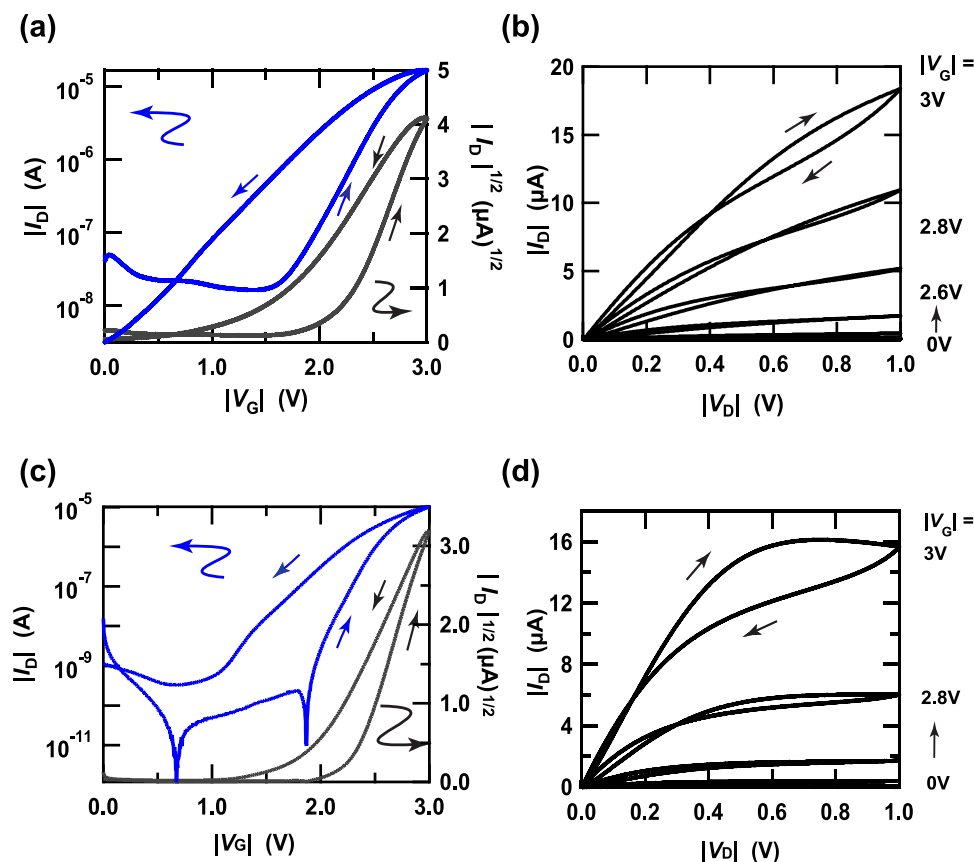


Figure 6. (a) Transfer and (b) output curves of a [10]phenacene EDL FET. (c) Transfer and (d) output curves of an [11]phenacene EDL FET.

sample	μ ($\text{cm}^2\text{V}^{-1}\text{s}^{-1}$)	$ V_{th} $ (V)	ON/OFF	S (V/decade)	L (μm)	W (μm)
#1	1.4	2.35	1.3×10^3	5.1×10^{-1}	100	600
#2	3.2	2.61	4.1×10^3	1.9×10^{-1}	100	214
#3	3.3	2.12	5.2×10^2	1.4	100	450
#4	3.4	2.22	1.5×10^3	8.9×10^{-1}	100	583
#5	4.2	2.18	1.0×10^3	4.0×10^{-1}	150	250
average	3(1)	2.3(2)	$2(1) \times 10^3$	$7(5) \times 10^{-1}$	—	—

Table 3. FET parameters of a [10]phenacene EDL FET with bmim [PF6]ionic liquid. The parameters for each device (each sample number) was determined from the forward transfer curve.

sample	μ ($\text{cm}^2\text{V}^{-1}\text{s}^{-1}$)	$ V_{th} $ (V)	ON/OFF	S (V/decade)	L (μm)	W (μm)
#1	4.6×10^{-1}	2.27	2.8×10^6	1.42×10^{-1}	100	286
#2	1.8	2.41	6.0×10^6	1.36×10^{-1}	100	232
#3	2.6	2.30	1.0×10^7	1.01×10^{-1}	100	214
#4	3.1×10^{-1}	2.11	5.4×10^4	2.29×10^{-1}	100	563
#5	2.8×10^{-1}	2.45	1.8×10^6	2.06×10^{-1}	100	525
average	1(1)	2.3(1)	$4(4) \times 10^6$	$1.6(5) \times 10^{-1}$	—	—

Table 4. FET parameters of an [11]phenacene EDL FET with bmim [PF6]ionic liquid. The parameters for each device (each sample number) was determined from the forward transfer curve.

The monotonic increase in c against n is reasonable because of the elongation of the long axis of the molecule. The decrease in band gap against n (Fig. 4b) is reasonably explained by the elongation of molecules. Admittedly, the band gaps of 2.96 and 2.95 eV for [10]phenacene and [11]phenacene are smaller than that, 3.18 eV, of [5]

phenacene (picene) determined in this study. The values of these band gaps are much larger than the 1.84 eV of pentacene³⁹, indicating that these molecules are still stable for photo-irradiation in air. This implies that the band gap of an armchair-shaped molecule (*i.e.*, [n]phenacene) changes little with the elongation of molecule, which should be favorable for device application.

As seen from Fig. 3e, the ϕ value becomes smaller with increasing n up to 10, which is explained by the increase in π - π interaction caused by the increase in C atoms (or extension of the π -framework). As suggested in ref.²⁸, the van der Waals interaction between phenacene molecules is probably produced by both the π - π interaction through the $2p_z$ orbitals of C and the CH... π interaction, leading to the herringbone stacking of phenacene molecules in the crystals. The π - π interaction should increase because of the extended benzene network, *i.e.*, the increase in the number of C atoms as described above. The CH... π interaction should slowly decrease because of the decrease in the ratio of H atoms to C atoms; 0.636 for picene (n = 5) to 0.571 for [10]phenacene (n = 10) and 0.565 for [11]phenacene (n = 11). Consequently, the ϕ value should decrease slowly because of the decrease in the above ratio. Admittedly, the ϕ gradually decreases up to n = 10, but it rapidly increases at only n = 11 ($\phi = 45^\circ$), despite the monotonic decrease in the H/C ratio. The reason is still unclear.

Previous reports of the μ value versus n in phenacene single-crystal FETs showed a straightforward increase in μ up to n = 9, which was reasonably explained by the increase in overlap (π - π interaction) between $2p_z$ orbitals in C atoms²⁸. However, the μ -n plot (n = 5 to 11) in phenacene thin-film FET showed no significant relationship between μ and n²⁸. This is probably due to the presence of extrinsic factors other than π - π interaction between phenacene molecules in a thin film, *i.e.*, the crystallinity and presence of defects in thin films may significantly affect the μ value. In this study, we could not obtain single crystals of [10]phenacene and [11]phenacene for the construction of a single-crystal FET, so the relation between μ and n in a phenacene single-crystal FET could not be obtained.

However, the synthesis of [10]phenacene and [11]phenacene molecules allowed the clarification of the behavior of extremely extended π -network molecules as well as their usability in an FET. Moreover, the [10]phenacene and [11]phenacene EDL FETs showed the averaged μ as high as $3(1) \text{ cm}^2 \text{ V}^{-1} \text{ s}^{-1}$ and $1(1) \text{ cm}^2 \text{ V}^{-1} \text{ s}^{-1}$, which is relatively high. The EDL FETs' high performance was also observed in [8]phenacene thin film FET²⁶, probably owing to the high density of carriers accumulated, which would lead to the lowering of contact resistance between source-drain electrodes and active layer.

Unfortunately, no single-crystal FETs using these molecules was fabricated in this study because of the difficulty of making single crystals suitable for FET devices. Therefore, a straightforward increase in μ against n was not recorded in this study, although it is obtained in the single crystal FET with [n]phenacene (n = 5–9). However, p-channel normally-off FET properties have been shown using thin films of these molecules, which does suggest a high potential of [10]phenacene and [11]phenacene for use in practical FET devices. Pursuing the extension of benzene networks in polycyclic aromatic hydrocarbons is currently one of the most important challenges in chemistry and materials science, as well as organic electronics. This work would open the avenue for pursuing chemistry/materials science of extended benzene network molecules (or phenacene molecules), and their application toward organic electronics.

Methods

Experimental details of syntheses of [10]phenacene and [11]phenacene. Compounds **1**³⁴, **4**²⁸, **6**³⁵, and **9**²⁶ were prepared according to the previously reported procedures. A mixture of 4-methylpicene **1** (398 mg, 1.36 mmol), *N*-bromosuccinimide (NBS, 290 mg, 1.63 mmol), and benzoyl peroxide (BPO, 75%, 22 mg, 0.07 mmol) in chlorobenzene (150 ml) was heated at 110 °C for 22 h. The solvent was removed under reduced pressure and the residue was successively washed with toluene and MeCN. The crude product was recrystallized from *o*-dichlorobenzene to afford 4-(bromomethyl)picene **2** (338 mg, yield of 67%). The obtained compound **2** was heated with triphenylphosphine (286 mg, 1.09 mmol) at 110 °C in *N,N*-dimethylformamide (DMF, 30 ml) overnight. The precipitated product was collected and recrystallized from a CHCl₃-toluene mixture to afford phosphonium salt **3** as pale brown solid (mp > 300 °C, 576 mg, yield of 91%). Physical data are shown in Supplementary Information.

To a solution of phosphonium salt **3** (190 mg, 0.30 mmol) and aldehyde **4** (77 mg, 0.30 mmol) in CH₂Cl₂ (30 ml) was added tetrabutylammonium hydroxide (Bu₄NOH; 1 M in MeOH, *i.e.*, 0.50 mmol in 0.5 ml). The solution was stirred at room temperature for 1 h, and the precipitated diarylethene **5** (135 mg, yield of 85%) was collected and successively washed with CH₂Cl₂ and toluene. This product was used in the following photoreaction without purification. A solution of diarylethene **5** (42.5 mg, 0.11 mmol) and a small portion of I₂ in 700 ml of boiling *o*-dichlorobenzene was irradiated with black-light lamps (6 × 15 W) for 15 min. After light irradiation, a precipitate was formed, which was collected and washed with toluene to afford [10]phenacene as off-white plates. This photoreaction was twice repeated to obtain a [10]phenacene powder sample (71 mg, total yield of 71% in two photoreactions).

A mixture of 1, 8-dimethylphenanthrene (1.03 g, 50.0 mmol), NBS (1.78 g, 10.0 mmol), and BPO (162 mg, 0.5 mmol) in CCl₄ (70 ml) was refluxed for 16 h. The solvent was removed and the residue was washed with MeOH to afford dibromide **7** as colourless solid (mp 180–188 °C, 1220 mg, yield of 67%).

A solution of dibromide **7** (910 mg, 2.5 mmol) and triphenylphosphine (1.44 g, 5.5 mmol) in toluene (50 ml) was refluxed for 18 h. The precipitate formed was collected and washed with toluene to afford bis-phosphonium salt **8** as colourless solid (mp > 280 °C, decomposed, 2160 mg, yield of 97%). Physical data appear in Supplementary Information.

To a solution of bis-phosphonium salt **8** (222 mg, 0.25 mmol) and aldehyde **9** (103 mg, 0.50 mmol) in CH₂Cl₂ (40 ml) was added a MeOH solution of tetrabutylammonium hydroxide (1 M, *i.e.*, 2.0 mmol for 2.0 ml), and the solution was stirred at room temperature for 14 h. The precipitated product (A) was collected and successively

washed with CH_2Cl_2 and MeOH. The filtrate was concentrated and the residue (B) was washed with MeOH. The obtained products, A and B, were combined to provide diene **10** (127 mg, yield of 87%) which was used in the following photoreaction without purification.

A boiling *o*-dichlorobenzene solution (700 ml) containing diene **10** (115 mg, 0.20 mmol) and small portion of I_2 was irradiated with black-light lamps ($6 \times 15 \text{ W}$) for 1 h. The precipitated product was collected and washed with *o*-dichlorobenzene to afford [11]phenacene as a pale brown solid (92 mg, yield of 79%).

Characterization of [10]phenacene and [11]phenacene. The MALDI-TOF MS spectrum was measured using a Bruker Autoflex mass spectrometer. The XRD patterns of the thin films of [10]phenacene and [11]phenacene were measured using a RIGAKU SMARTLAB-PRO with $\text{Cu K}\alpha$ source (wavelength of 1.5418 Å), and the XRD patterns of crystalline powders of [10]phenacene and [11]phenacene were measured at BL12B2 of SPring-8 with an X-ray beam of wavelength = 0.68865 Å. The AFM images of thin films of [10]phenacene and [11]phenacene were recorded with a measurement system (SII Nano Technology SPA400). The UV-VIS absorption spectra of thin films of [10]phenacene and [11]phenacene were measured using a UV-VIS spectrometer (JASCO V-670 iRM EX).

STM experiments were performed in an ultra-high vacuum of 10^{-10} Torr using a modified Unisoku USM1300 system. [10]phenacene molecules were thermally deposited at $\sim 530 \text{ K}$ at a rate of 0.1 molecular layers per minute onto a clean Au(111) surface. The substrate was kept at room temperature. After sample transfer, the STM imaging was conducted at 77 K with a bias voltage applied to the sample, *i.e.*, positive voltages refer to tunnelling into unoccupied sample states.

Preparation of FET devices using thin films of [10]phenacene and [11]phenacene and measurement of FET characteristics. The surfaces of the SiO_2 gate dielectrics used for [10]phenacene and [11]phenacene thin-film FETs were treated with 1, 1, 1, 3, 3, 3-hexamethyldisilazane (HMDS) to produce a hydrophobic surface, as is described elsewhere²³. The thin films were formed on the SiO_2 gate dielectric by thermal deposition under a vacuum of 10^{-6} Torr, with the substrate kept at room temperature during thermal deposition. Thin films 60 nm thick of [10]phenacene and [11]phenacene were prepared by thermal deposition under a vacuum of 10^{-6} Torr. Au source/drain electrodes 50 nm thick were formed on the thin films by thermal deposition under 10^{-6} Torr. 3 nm thick F_4TCNQ was inserted between the thin films and the source/drain electrodes to reduce contact resistance. The FET device with an SiO_2 gate dielectric employed a top-contact and bottom gate structure (Fig. S1a). The above thin films of [10]phenacene and [11]phenacene were used for XRD and AFM measurements.

The EDL polymer sheet was used for the gate dielectric of [10]phenacene and [11]phenacene EDL FETs; the polymer sheet was prepared using [1-butyl-3-methylimidazolium][hexafluorophosphate] ($\text{bmim}[\text{PF}_6]$) and poly(vinylidene fluoride-co-hexafluoropropylene). Details of its synthesis are given in ref.²¹. As described in the Results section, the gate voltage was applied from a side-gate electrode in thin-film EDL FETs, *i.e.*, this device employed a side-gate top-contact structure (Fig. S1d).

The FET characteristics were recorded using a semiconductor parameter analyzer (Agilent B1500A) for the FET devices in an Ar-filled glove box. The capacitance per area, C_o , was measured using a precision LCR meter (Agilent E4980A). The C_o value for evaluation of FET performance was determined by extrapolation of the capacitance measured at 20 Hz–1 kHz to 0 Hz. The C_o values of SiO_2 and EDL gate-dielectric (polymer sheet) at 0 Hz were 8.34 nF cm^{-2} and $8.01 \mu\text{F cm}^{-2}$, respectively. All FET properties were evaluated from the forward transfer curves at saturation regime.

References

- Iijima, S. Helical microtubules of graphitic carbon. *Nature* **354**, 56–58 (1991).
- Sariciftci, N. S., Smilowitz, L., Heeger, A. J. & Wudl, F. Photoinduced electron transfer from a conducting polymer to buckminsterfullerene. *Science* **258**, 1474–1476 (1992).
- Hebard, A. F. *et al.* Superconductivity at 18 K in potassium-doped C_{60} . *Nature* **350**, 600–601 (1991).
- Novoselov, K. S. *et al.* Electric field effect in atomically thin carbon films. *Science* **306**, 666–669 (2004).
- Geim, A. K. & Novoselov, K. S. The rise of graphene. *Nature Mater.* **6**, 183–191 (2007).
- Novoselov, K. S. *et al.* Two-dimensional gas of massless Dirac fermion in graphene. *Nature* **438**, 197–200 (2005).
- Neto, A. H. C., Guinea, F., Peres, N. M. R., Novoselov, K. S. & Geim, A. K. The electronic properties of graphene. *Rev. Mod. Phys.* **81**, 109–162 (2009).
- Friend, R. H. *et al.* Electroluminescence in conjugated polymers. *Nature* **397**, 121–128 (1999).
- Dimitrakopoulos, C. D. & Malenfant, P. R. L. Organic thin film transistors for large area electronics. *Adv. Mater.* **14**, 99–117 (2002).
- Podzorov, V., Sysoev, S. E., Loginova, E., Pudalov, V. M. & Gershenson, M. E. Single-crystal organic field effect transistors with the hole mobility $\sim 8 \text{ cm}^2/\text{Vs}$. *Appl. Phys. Lett.* **83**, 3504–3506 (2003).
- de Boer, R. W. I., Klapwijk, T. M. & Morpurgo, A. F. Field-effect transistors on tetracene single crystals. *Appl. Phys. Lett.* **83**, 4345–4347 (2003).
- Forrest, S. R. The path to ubiquitous and low-cost organic electronic appliances on plastic. *Nature* **428**, 911–918 (2004).
- Newman, C. R. *et al.* Introduction to organic thin film transistors and design of n-channel organic semiconductors. *Chem. Mater.* **16**, 4436–4451 (2004).
- Hoppe, H. & Sariciftci, N. S. Organic solar cells: An overview. *J. Mater. Res.* **19**, 1924–1945 (2004).
- Yamamoto, T. & Takimiya, K. Facile synthesis of highly π -extended heteroarenes, dinaphtho[2, 3-*b*: 2', 3'-*f*]chalcogenopheno[3, 2-*b*]chalcogenophenes, and their application to field-effect transistors. *J. Am. Chem. Soc.* **129**, 2224–2225 (2007).
- Takeya, J. *et al.* Very high-mobility organic single-crystal transistors with in-crystal conduction channels. *Appl. Phys. Lett.* **90**, 102120 (2007).
- Thompson, B. C. & Fréchet, J. M. J. Organic photovoltaics – polymer-fullerene composite solar cells. *Angew. Chem. Int. Ed.* **47**, 58–77 (2008).
- Kawasugi, Y. *et al.* Strain-induced superconductor/insulator transition and field effect in a thin single crystal of molecular conductor. *Appl. Phys. Lett.* **92**, 243508 (2008).

19. Okamoto, H. *et al.* Air-assisted high-performance field-effect transistor with thin films of picene. *J. Am. Chem. Soc.* **130**, 10470–10471 (2008).
20. Chang, Y.-J., Yang, S.-H. & Hsu, C.-S. Synthesis of conjugated polymers for organic solar cell applications. *Chem. Rev.* **109**, 5868–5923 (2009).
21. Kubozono, Y. *et al.* Transistor application of phenacene molecules and their characteristics. *Eur. J. Inorg. Chem.* **2014**, 3806–3819 (2014).
22. Yuan, Y. *et al.* Ultra-high mobility transparent organic thin film transistors grown by an off-centre spin-coating method. *Nature Commun.* **5**, 3005 (2014).
23. Okamoto, H. *et al.* Transistor application of alkyl-substituted picene. *Sci. Rep.* **4**, 5048 (2014).
24. Mitsuhashi, R. *et al.* Superconductivity in alkali-metal-doped picene. *Nature* **464**, 76–79 (2010).
25. Kubozono, Y. *et al.* Metal-intercalated aromatic hydrocarbons: a new class of carbon-based superconductors. *Phys. Chem. Chem. Phys.* **13**, 16476–16493 (2011).
26. Okamoto, H. *et al.* An extended phenacene-type molecule, [8]phenacene: synthesis and transistor application. *Sci. Rep.* **4**, 5330 (2014).
27. Shimo, Y. *et al.* Transistors fabricated using the single crystals of [8]phenacene. *J. Mater. Chem. C* **3**, 7370–7378 (2015).
28. Shimo, Y. *et al.* Synthesis and transistor application of the extremely extended phenacene molecule, [9]phenacene. *Sci. Rep.* **6**, 21008 (2016).
29. Mallory, F. B. *et al.* Phenacenes: a family of graphite ribbons. 2. Syntheses of some [7]phenacenes and an [11]phenacene by stilbene-like photocyclizations. *J. Am. Chem. Soc.* **119**, 2119–2124 (1997).
30. Mallory, F. B. *et al.* Phenacenes: a family of graphite ribbons. Part 3: Iterative strategies for the synthesis of large phenacenes. *Tetrahedron* **57**, 3715–3724 (2001).
31. Moreira, T. S. *et al.* Tetracarboxy-functionalized [8]-, [10]-, [12]-, and [14]phenacenes. *Eur. J. Org. Chem.* **2017**, 4548–4551 (2017).
32. Mallory, F. B., Butler, K. E., Evans, A. C. & Mallory, C. W. Phenacenes: a family of graphite ribbons. 1. Syntheses of some [7]phenacenes by stilbene-like photocyclizations. *Tetrahedron Lett.* **37**, 7173–7176 (1996).
33. Mallory, F. B. *et al.* Phenyl groups versus *tert*-butyl groups as solubilizing substituents for some [5]phenacenes and [7]phenacenes. *J. Org. Chem.* **78**, 2040–2045 (2013).
34. Okamoto, H. *et al.* Efficient synthetic photocyclization for phenacenes using a continuous flow reactor. *Chem. Lett.* **43**, 994–996 (2014).
35. Rubin, M. B. & Welner, S. Synthesis of 1, 8-(6', 7'-dioxododecamethylene)phenanthrene. *J. Org. Chem.* **45**, 1847–1852 (1980).
36. Chen, S.-W., Sang, I.-C., Okamoto, H. & Hoffmann, G. Adsorption of phenacenes on a metallic substrate: Revisited. *J. Phys. Chem. C* **121**, 11390–11398 (2017).
37. Kawasaki, N., Kubozono, Y., Okamoto, H., Fujiwara, A. & Yamaji, M. Trap states and transport characteristics in picene thin film field-effect transistor. *Appl. Phys. Lett.* **94**, 043310 (2010).
38. Lee, X. *et al.* Quantitative analysis of O₂ gas sensing characteristics of picene thin film field-effect transistors. *Organic Electronics* **11**, 1394–1398 (2010).
39. Costa, J. C. S., Taveira, R. J. S., Lima, C. F. R. A. C., Mendes, A. & Santos, L. M. N. B. F. Optical band gaps of organic semiconductor materials. *Opt. Mater.* **58**, 51–60 (2016).

Acknowledgements

This study was partly supported by Grants-in-Aid (26105004, 17K05976 and 17K05500) from MEXT, and the JST-ACT-C project of the Japan Science and Technology Agency (No. JPMJCR 12YW), and by the Program for Promoting the Enhancement of Research Universities. The XRR measurements at SPring-8 were performed under proposals No. 2017B4133 and No. 2017B4138. The STM measurements were funded by the Ministry of Science and Technology R.O.C. through grants 105-2112-M-007-022-MY3 and 106-2923-M-007-001-MY4.

Author Contributions

Y.K. designed this research project and supervised experiments. H.O. synthesized [10]phenacene and [11]phenacene, and H.O., S.H., Y.T., S.G., H.S., Y.F.L. and H.I. characterized their samples using various spectroscopic, imaging and diffraction techniques. S.H. fabricated the FET devices and measured their FET characteristics. Y.H.Y., L.U.L., C.W.C. and G.H. conducted the STM experiments. H.O., S.H., R.E., H.G. (Okayama) and Y.K. discussed the scientific implications of the data obtained. Y.K. wrote this paper with the aid of discussions with H.O., S.H., R.E. and H.G.

Additional Information

Supplementary information accompanies this paper at <https://doi.org/10.1038/s41598-019-39899-4>.

Competing Interests: The authors declare no competing interests.

Publisher's note: Springer Nature remains neutral with regard to jurisdictional claims in published maps and institutional affiliations.



Open Access This article is licensed under a Creative Commons Attribution 4.0 International License, which permits use, sharing, adaptation, distribution and reproduction in any medium or format, as long as you give appropriate credit to the original author(s) and the source, provide a link to the Creative Commons license, and indicate if changes were made. The images or other third party material in this article are included in the article's Creative Commons license, unless indicated otherwise in a credit line to the material. If material is not included in the article's Creative Commons license and your intended use is not permitted by statutory regulation or exceeds the permitted use, you will need to obtain permission directly from the copyright holder. To view a copy of this license, visit <http://creativecommons.org/licenses/by/4.0/>.

© The Author(s) 2019